Journal Pre-proof

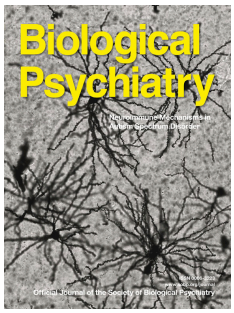

40 Hz Auditory Steady State Responses in Schizophrenia: Towards a Mechanistic Biomarker for Circuit Dysfunctions and Early Detection and Diagnosis

Tineke Grent-'t-Jong, Ph.D., Marion Brickwedde, Ph.D., Christoph Metzner, Peter J. Uhlhaas, Ph.D.

PII: S0006-3223(23)01210-6

DOI: https://doi.org/10.1016/j.biopsych.2023.03.026

Reference: BPS 15174

To appear in: *Biological Psychiatry*

Received Date: 15 February 2023

Revised Date: 21 March 2023

Accepted Date: 30 March 2023

Please cite this article as: Grent-'t-Jong T., Brickwedde M., Metzner C. & Uhlhaas P.J., 40 Hz Auditory Steady State Responses in Schizophrenia: Towards a Mechanistic Biomarker for Circuit Dysfunctions and Early Detection and Diagnosis, *Biological Psychiatry* (2023), doi: https://doi.org/10.1016/j.biopsych.2023.03.026.

Number of Tables: 1

Number of Figures: 4

Number of Suppl. Figures: -

40 Hz Auditory Steady State Responses in Schizophrenia: Towards a Mechanistic Biomarker for Circuit Dysfunctions and Early Detection and Diagnosis

Grent-'t-Jong, Tineke, Ph.D.[1], Brickwedde, Marion Ph.D.[1], Metzner, Christoph[2,3] & Uhlhaas, Peter J., Ph.D.[1,4]

1. Department of Child and Adolescent Psychiatry, Charité Universitätsmedizin, Berlin, Germany
2. Neural Information Processing Group, Institute of Software Engineering and Theoretical Computer Science, Technische Universität Berlin, Berlin, Germany
3. School of Physics, Engineering and Computer Science, University of Hertfordshire, Hatfield, UK
4. Institute of Neuroscience and Psychology, University of Glasgow, Glasgow, U.K.

Running Head title: Auditory 40-Hz Steady-State Responses in Schizophrenia

Keywords: Schizophrenia, 40 Hz Auditory Steady State, Biomarker, Excitation/Inhibition Balance, Oscillations

Correspondence:

Prof. Peter J. Uhlhaas
Department of Child and Adolescent Psychiatry
Augustenburger Platz 1
Charité Universitätsmedizin
Berlin 13353
Germany
Email: peter.uhlhaas@charite.de
Tel: +49 30 450 516 193

Abstract

There is converging evidence that 40 Hz Auditory Steady State Responses (ASSRs) are robustly impaired in schizophrenia and could constitute a potential biomarker for characterizing circuit dysfunctions as well as enable early detection and diagnosis. In the current paper, we provide an overview of the mechanisms involved in 40 Hz ASSRs, drawing on computational, physiological and pharmacological data with a focus on parameters modulating the balance between excitation/inhibition. We will then summarize findings from electro- and magnetoencephalographical studies in clinical high-risk for psychosis participants, first-episode psychosis and schizophrenia patients to identify the pattern of deficits across illness-stages, the relationship with clinical variables and prognostic potential. Finally, data on genetics and developmental modifications will be reviewed, highlighting the importance of late modifications of 40 Hz ASSRs during adolescence which are closely related to the underlying changes in gamma-aminobutyric acid interneurons. Together, our review suggests that 40 Hz ASSRs may constitute an informative electrophysiological approach to characterize circuit dysfunctions in psychosis that could be relevant for the development of mechanistic biomarkers.

Introduction

The identification of non-invasive biomarkers for diagnosis and prognosis is a fundamental challenge in current schizophrenia (ScZ) research (1). Importantly, biomarkers should ideally allow insights into the underlying pathophysiological mechanisms and facilitate links to pre-clinical research (2). One potential candidate is the 40 Hz Auditory Steady-State Response (ASSR). Steady-state responses (SSRs) reflect stimulus-rate dependent, evoked activity to constant periodic stimuli in different sensory modalities that can be detected using electro- and magnetoencephalography (EEG/MEG). ASSRs show a peak frequency around 40 Hz in humans (3) in contrast to other sensory modalities, such as visual SSRs (4).

40 Hz ASSRs were investigated for the first time in ScZ patients by Kwon et al. (5) using EEG, demonstrating reduced power and phase delay to 40 Hz stimulation. These findings provided further support for the hypothesis that neural circuits were compromised in ScZ to generate oscillations in the gamma-band (30-100 Hz) (6). During normal brain functioning, gamma-band oscillations have been proposed to facilitate coordination of distributed neuronal activity in neuronal networks to support the generation of perception and cognition (7) and are accordingly a candidate mechanism for the pervasive sensory and cognitive deficits in ScZ (8).

The initial findings by Kwon et al. (5) have been replicated by several groups using both EEG and MEG (9-11). In addition, more recent studies have examined 40 Hz ASSRs in participants at clinical high-risk for psychosis (CHR-P) and first-episode psychosis (FEP) patients (12, 13), raising the possibility that 40 Hz ASSRs could be used for early detection and diagnosis of early-stage psychosis.

Despite the extensive evidence on 40 Hz ASSR deficits in ScZ, several questions remain regarding their significance and interpretation. Therefore, the goal of this paper is to provide a state-of-the art overview on the 40 Hz ASSRs as a mechanistic biomarker for elucidating circuit dysfunctions in ScZ as well as for early detection and diagnosis. Accordingly, we will

summarize the mechanisms underlying 40 Hz ASSRs, drawing on computational, physiological and pharmacological perspectives. This will be followed by an overview of current studies in CHR-P participants, FEP-groups and ScZ-patients. Finally, evidence from genetics as well as recent studies on the 22q11.2 deletion syndrome (22q11.2DS) will be reviewed together with data on developmental modifications, followed by recommendations for future research.

Generators Underlying 40 Hz ASSRs in Human and Animal Electrophysiology

Current EEG and MEG-studies interpret 40 Hz ASSRs as a probe for measuring the resonance frequency of auditory circuits. However, while initial findings focused on auditory regions as the main areas involved in the generation of the 40 Hz ASSR, in particular the medial Heschl's gyrus (14, 15), more recent work has suggested that 40 Hz ASSRs involve a more extensive network.

Evidence for the contribution of frontal generators towards 40 Hz ASSRs in humans comes from MEG/EEG (16, 17) as well as from intracranial recordings (18). In addition, 40 Hz ASSRs have been observed in parietal areas (14) and in the inferior colliculus (19). Tada et al. (18) analyzed high-density electrocorticography in response to ASSRs at 20, 30, 40, 60, 80, 120, and 160 Hz using two common techniques to analyze steady-state activity, intertrial phase coherence (ITPC) (20) and spectral power estimates. The first refers to the consistency of phase-angles across trials, therefore reflecting only evoked activity. The latter encompasses both evoked activity and induced components, of which the timing can differ between trials. Modulation of ITPC and spectral power were maximal at 40 Hz stimulation and were distributed across temporal, parietal, and frontal cortices.

In addition, there is evidence for a role of the thalamus, in particular the medial geniculate body (MGB), in the generation of 40 Hz ASSRs from MEG/EEG, PET and fMRI-data (12, 19, 21).

These findings were corroborated by a study showing that electrical stimulation of thalamic neurons evoked gamma-band activity around 40 Hz in auditory cortex (22). Moreover, recent work has shown that generators extend to additional subcortical areas, including hippocampus (12) and the brainstem (15).

Enter Figure 1 about here

Circuit Mechanisms of 40 Hz ASSRs: E/I Balance Parameters

Unlike transient evoked potentials, SSRs require a high temporal resolution for coordinated signal integration as well as transmission and processing, especially in higher-frequency ranges (23). Initial efforts focused on disclosing whether SSRs simply constitute a summation of event-related potentials (ERPs) or whether they reflect the entrainment of rhythmic oscillatory activity. While some studies supported to the summation hypothesis(24, 25), it is more likely that both models are non-exclusive and interacting to produce the ASSR response.

As such, it has been proposed that early transient components of the ASSR response may reflect ERP processes, while late-latency, sustained responses reflect rhythmic activity (11, 16). This theory is supported by evidence indicating that ITPC is larger for the late sustained 40 Hz ASSRs (150-500 ms) compared to ITPC-modulation between 0-50 ms (12, 26), suggesting that sustained rhythmic activity may be only observed after the early evoked component. In this context, it is important to highlight that neural oscillations reflect synchronous, rhythmic activity of neuronal ensembles that occurs in a circumscribed frequency range and are sustained over several cycles (27). Accordingly, neural oscillations need to be distinguished from broad-

band power changes, transient responses as well as aperiodic activity (28) and recent methods have been introduced to separate these processes (29).

Gamma-band oscillations emerge from the balance between excitation and inhibition (E/I-balance) in neural networks (30). Specifically, the time-constants of inhibitory postsynaptic potentials (IPSPs) of GABAergic parvalbumin-positive (PV+) interneurons are ideally suited to generate 40 Hz rhythms (31). This has been shown for instance through hippocampal excitation of PV+ interneurons by means of N-methyl-D-aspartate receptors (NMDA-Rs), which resulted in 40 Hz transient oscillatory responses in pyramidal cells (32, 33).

PV+ interneurons mainly target the perisomatic region of pyramidal cells and can therefore control their output effectively as opposed to Somatostatin-Expressing (SST+) interneurons that mainly inhibit the apical dendrite (34). Computational studies have further demonstrated that these anatomical and electrophysiological properties PV+ interneurons are crucial for the generation of gamma-band oscillations and that several key E/I-balance parameters determine their power and coherence (35). Moreover, the strength of exerted inhibition, which in turn is dependent on the strength of NMDA-R activation as well as the maximal conductance of the GABAergic synapses, also crucially influences 40 Hz ASSR power (36-39).

Further evidence for the role of E/I-balance parameters in the generation of 40 Hz ASSRs comes from pharmacological studies. In human EEG-recordings, the NMDA-R antagonist ketamine has been associated with an increase in power of the 40 Hz ASSRs (40). In contrast, administration of the NMDA-R antagonist MK 801 into the medial geniculate body (MGB) in mice was associated with reduced 40 Hz ASSRs in auditory cortex, without affecting the early transient response (41). Such diverging findings could be explained by different locations and dosages of drug administration. For instance, Sirano et al. (42) showed that NMDA-R channel occupancy is related to the modulation of both power and phase-locking of 40 Hz ASSRs, with lower ketamine dosages causing an increase in spectral power and ITPC while higher doses caused decreased 40 Hz ASSRs.

Similarly, there is emerging evidence that GABAergic neurotransmission modulates 40 Hz ASSRs. Increasing inhibition via administration of the GABAA agonist muscimol results in increased power and phase-locking of 40 Hz ASSRs in humans (43). Moreover, selective PV+ interneuron excitation using optogenetic stimulation in the basal forebrain in rats increased ASSR-responses in auditory cortex only when stimulating at 40 Hz but not at other frequencies (44). Accordingly, these data indicate that modulation of both power and ITPC-values of 40 Hz ASSRs are the sensitive marker for E/I-balance alterations that could allow the identification of circuit mechanisms in ScZ. In particular, both PV+ interneuron activation as well as the excitatory drive mediated through NMDA-Rs have a mechanistic impact on 40 Hz ASSRs.

Enter Figure 2 about here

40 Hz ASSRs in Schizophrenia: Pattern of Deficits and Correlations with Clinical Variables

40 Hz ASSRs have been investigated in approximately 40 studies in ScZ patients using both EEG and MEG (for a recent review see (44)). The large majority of studies have reported a reduction in both ITPC and power of 40 Hz ASSRs with medium-level effect sizes ((9) but see (45, 46)). This pattern is consistent with evidence from other sensory and cognitive paradigms in ScZ (8), suggesting that neural circuits involved in the generation of high-frequency oscillations are impaired.

So far, however, studies have focused almost exclusively on the analysis of sensor-level data and source-localization of auditory regions as the origin of 40 Hz ASSRs deficits. Accordingly, it is unclear which areas are fundamentally implicated beyond auditory cortex given the contribution of extensive cortical and subcortical regions towards the generation of 40 Hz ASSRs (12, 18). Koshiyama et al. (47) applied a Granger causality analysis, a functional connectivity measure, to assess the propagation of 40 Hz ASSRs across cortical sources in a large sample of ScZ patients and controls. ScZ patients showed a complex pattern of increased and decreased connectivity across the early transient as well as during the later sustained responses that involved temporal and frontal brain regions.

In ScZ patients, there is evidence for a reduction in both the early transient and sustained 40 Hz ASSRs (48) which may, however, differ across early vs. later illness stages (49). In addition, Kwon et al. (5) reported a delay between click onset and the subsequent negative peak in band filtered time-domain EEG data. This finding was replicated by Roach et al. (50) (see also (51)), highlighting that the phase delay deficit in ScZ patients was associated with a significantly larger effect size than both spectral power and ITPC-reductions.

An important aspect concerns the specificity of ASSR deficits towards 40 Hz stimulation. While auditory cortices during normal brain functioning respond preferentially to 40 Hz ASSRs (18), there is consistent evidence that impairments in ScZ extend to other frequencies. Thus, ASSR deficits have also been observed at 80 Hz but not at 20 Hz or 30 Hz (52). In addition, several studies have shown that ASSRs at delta (1-4 Hz) (53) but also theta-bands (4-7 Hz) are reduced in ScZ as well (54). During normal brain functioning, there is evidence that low and high-frequency oscillations interact, for example, the amplitude of gamma-band activity can be modulated by the phase of low-frequency (delta/theta-band) oscillations (55). However, studies that investigated cross-frequency coupling showed that 40 Hz ASSR deficits were not related to lower frequencies in ScZ (56, 57).

Among the clinical correlates, correlations between increased 40 Hz ASSRs and elevated positive symptoms, especially auditory hallucinations (58, 59), have been reported which, however, has not been confirmed by other studies (52). In addition, Ogy et al. (60) examined whether 40 Hz ASSRs differentiated ScZ-patients who did not respond to standard antipsychotics (treatment-resistant schizophrenia (TRS)) vs. a non-TRS group. Evoked power during 40 Hz ASSRs was only impaired in the TRS group compared to controls. However, no differences were found between TRS and non-TRS ScZ-patients in 40 Hz ASSR power.

Given that gamma-band oscillations have been proposed to underlie impaired cognitive and sensory processes in ScZ (8), correlations between deficits in 40 Hz ASSRs, cognition and possibly also functional impairments can be expected. Robust relationships with cognitive deficits have not been demonstrated so far (12, 56, 61). In regards to functional impairments, there is preliminary evidence that reduced 40 Hz ASSRs correlate with lower functional status in ScZ patients (61).

Finally, several studies have examined the relationship between anatomical alterations, especially gray matter (GM) volume, and 40 Hz ASSRs in ScZ. Thus, there is evidence that GM-reductions in the auditory cortex correlate with decreased 40 Hz ASSRs (62). A study by Du et al. (63) that linked fMRI resting-state data to sensor level 40 Hz ASSRs suggested, however, that a network of brain areas consisting of temporal, medial prefrontal cortex and postcentral/ precentral gyrus is associated with deficient 40 Hz ASSRs.

40 Hz ASSR Deficits in Early-Stage Psychosis

More recent work has investigated whether 40 Hz ASSR impairments are present during early-stage psychosis to address the potential as a biomarker for early detection and diagnosis (Table

1). This is particularly important as early intervention can modify the trajectory of patients with a first-episode of psychosis (FEP) (64) and there is an urgent need for biomarkers to stratify patients according to clinical outcomes and pathophysiological mechanisms (65).

Currently, several studies investigated 40 HZ ASSRs in FEP-patients (12, 13, 49, 58, 66-68), the majority of which reported robust impairments in both spectral power and ITPC while Bartolomeo et al. (68) and Coffman (58) found intact 40 Hz power. In regards to CHR-P participants, Lepock et al. (69) showed intact ITPC and 40 Hz ASSR power while Grent-'t-Jong et al. (12), Koshiyama et al. (66) and Tada et al. (49) found evidence for impaired 40 Hz ASSRs.

Grent-'t-Jong et al. (12) furthermore examined the question whether 40 Hz ASSRs could constitute a biomarker for clinical outcomes in CHR-Ps, such as persistence of attenuated psychotic symptoms (APS) and transition to psychosis. Source-reconstructed 40 Hz ASSRs revealed that both CHR-Ps and FEP-groups had an overlapping deficit in spectral power and ITPC in auditory cortex, hippocampus and thalamus. Importantly, both APS persistence and transition to psychosis were predicted by 40 Hz ASSRs deficits in the hippocampus, thalamus and superior temporal gyrus.

Several studies also examined associations between 40 Hz ASSRs, functioning and symptoms in early-stage psychosis. Similar to findings in established ScZ, however, correlations with functioning (12, 70), symptoms (12, 58) and cognitive impairments (12) were inconsistent across studies.

Enter Figure 3 about here

40 Hz ASSRs, Genetics and Brain Development

The heritability of ScZ is estimated at approximately 80% (71) and recent genome-wide associations studies (GWAS) have identified risk genes that impact on E/I-balance parameters (72). There is preliminary evidence that unaffected 1st degree relatives exhibit reductions in 40 Hz ASSRs (73). Moreover, computational modelling has shown the impact of common variants on 40 Hz ASSRs (74) (Figure 1), suggesting that 40 Hz ASSR deficits are closely linked to genetic risk and therefore could constitute an endophenotype. This possibility is consistent with data showing that 40 Hz ASSR deficits can also be found in conditions that are characterized by overlapping circuit dysfunctions and genetics, such as Bipolar Disorder (BPD) and Autism Spectrum Disorders (ASDs) (75-78).

More recent studies have examined the relationship between 40 Hz ASSR deficits in 22q11.2 deletion syndrome (22q11DS) (17, 79), which is a neurogenetic disorder that confers a 30%−40% lifetime risk for the development of psychosis (80). Several genes within the 22q11.2 region have been linked to glutamatergic and GABAergic neurotransmission (81) and disrupted migration and placement of cortical interneurons (82). Mancini et al. (17) examined 40 Hz ASSRs in EEG data in a sample of 22q11.2 deletion carriers and controls. Both power and ITPC of 40 Hz ASSRs as well as evoked theta-band power were impaired in deletion carriers. Gamma band spectral power reductions were particularly prominent in anterior cingulate cortex (ACC), posterior cingulate cortex (PCC), thalamus and the right primary auditory cortex. Moreover, 40 Hz ASSR deficits were pronounced in deletion carriers with psychotic symptoms and correlated with the reduction of GM in auditory cortex. Importantly, a linear increase of 40 Hz ASSR spectral power was observed from childhood to adulthood in healthy controls but not in deletion carriers.

There is convergent evidence that E/I-balance, such as PV+ interneurons and their excitatory inputs (83) as well as a GABAergic subunits (84), undergo important modifications during

adolescence, which could in turn could provide sensitive periods for risk factors, such as cannabis (85), but also interventions that could potentially modify and even restore existing circuit dysfunctions. A study by Mukherjee et al. (86) examined the possibility to modify PV+ interneuron functioning in a mouse model of 22q11DS during development. Adult mice with a deletion on chromosome 16 (Df(16)A(+/)were characterized by low PV+ interneuron plasticity as well as pronounced deficits in cognitive tasks and gamma-band oscillations. Importantly, cognitive dysfunction in LgDel+/ mice could be prevented permanently by dopaminergic D2-receptor antagonist treatment or by chemogenetic activation of PV+ interneurons during late adolescence.

Enter Figure 4 about here

40 Hz ASSR Deficits in Schizophrenia: Link to E/I-Balance Circuit Dysfunctions

Impaired gamma-band oscillations in ScZ have been linked to altered E/I-balance parameters, in particular PV+ interneurons deficits (87) as well NMDA-R hypofunctioning (88). The precise pattern and contributions of NMDA-Rs and GABAergic interneurons towards impaired gamma-band oscillations in ScZ remains unclear, however. One possibility is that circuit deficits are due to a primary dysfunction in inhibitory interneurons in ScZ (87). In addition, evidence exists that impaired inhibition could be the result of NMDA-R hypofunctioning on PV+ interneurons (89) or reduced NMDA-R drive on pyramidal cells (90).

A shift towards increased excitation as a result of NMDA-R hypofunctioning has been implicated in circuit dysfunctions in ScZ, in particular during early-stage psychosis (91). Ketamine, a NMDA-R antagonist, is associated with disinhibition in local (92) and large-scale

networks (90) and a dysregulation of gamma-band oscillations (93). Specifically, lower dosages of NMDA-R antagonists, which elicit psychomimetic effects in healthy volunteers, cause preferentially an upregulation of both 40 Hz ASSRs (40, 42) and spontaneous gamma-band oscillations (93, 94). However, this pattern is not consistent with the 40 Hz ASSR findings in both CHR-P/FEP and ScZ-patients (9, 10).

Increased, non-phase locked or induced gamma-band power consistent with NMDA-R hypofunctioning model has been shown to correlate with 40 Hz ASSRs ITPC deficits in ScZ (95). However, several studies that examined baseline activity during visual processing (12, 96) could not confirm that spontaneous gamma-band activity is increased. Accordingly, further studies are required to examine the significance of elevated spontaneous gamma-band activity and its relationship with stimulus-related oscillatory activity in ScZ.

Computational models have shown that decreased PV+ interneuron mediated inhibition as a result of either reduced expression of glutamic acid decarboxylase isoform 67kDa (GAD67) or a reduction of PV+ interneuron cell density leads to reduced 40 Hz ASSRs (36, 37), with PV+ basket cells being primarily responsible for the 40Hz ASSR results as opposed to other PV+ interneuron subclasses such as Chandelier cells (97). This reduction is a result of the weakened control of the inhibitory cells over the firing of the pyramidal cell population leading to reduced 40 Hz rhythms. In contrast, hypofunction of NMDA-Rs on PV+ interneurons is associated with a decreased excitability in inhibitory cells (39), which decreased their recruitment during 40 Hz oscillations and, therefore, results in a reduction of 40 Hz ASSR power (38, 97, 98). Overall, it is conceivable that 40 Hz ASSR deficits may result from a combination of several changes to excitatory and GABAergic neurotransmission in ScZ (37) (see Figure 2).

Adams et al. (99) applied dynamic causal modelling (DCM) to identify the contribution of diminished synaptic gain on pyramidal cells vs. diminished synaptic gain on interneurons towards circuit dysfunctions in ScZ. EEG-data during 40 Hz ASSRs, resting-state activity and a MMN-paradigm were analyzed and a canonical microcircuit neural mass model was

employed. The results strongly favored reduced synaptic gain on pyramidal cells which is consistent with recent post-mortem data (100) that have indicated that reductions in PV+ interneurons may constitute an adaptive response to decreased excitatory drive.

Thus, the current findings suggest that 40 Hz ASSRs deficits in ScZ may be compatible with altered E/I-balance parameters. Specifically, evidence from pharmacology, post-mortem and computational modelling converges on the notion that reduced 40 Hz ASSRs in ScZ could be the result of impaired PV+ interneuron functioning (44, 97). However, it is currently unclear whether this dysfunction is primary or secondary to an excitatory deficit.

While the concept of E/I imbalance has been useful to gain a first mechanistic understanding of circuit deficits in ScZ, current models of E/I balance should be extended to capture important aspects of the ASSR response and generation. For example, most models do not capture the diversity of cortical interneurons, with some exceptions (97, 101). Furthermore, modelling studies so far have assumed that the ASSR response can be considered a simple summation of ERPs and have not addressed the entrainment of ongoing intrinsic oscillations by periodic ASSR stimuli.

Recommendations for Future Research

40 Hz ASSRs are influenced by a number of experimental parameters that require careful consideration. Attention has been shown to be modulate 40 Hz ASSRs power in healthy controls (102) but not in FEPs (58) nor in ScZ patients (103). Accordingly, future studies need to examine and control more carefully differences in attention as a possible confound for 40 Hz ASSR deficits in ScZ.

Secondly, state-dependent variables, such as arousal, may impact the strength of 40 Hz ASSRs (104). This is supported by findings indicating that eyes-open versus eyes-closed conditions

modulate the strength 40 Hz ASSRs (105). It is currently uncear, however, whether these manipulations differ in ScZ or FEP-groups (67, 106). Finally, it has been argued that amplitude-modulated (AM) sounds, compared to click-trains, are more powerful in detecting late sustained 40 Hz impairments, whereas click-trains are most sensitive to detecting early-latency deficits (107). However, studies using click-train paradigms have shown sustained impairments for the duration of stimulation (9).

Regarding EEG/MEG analytic approaches, the consideration of baseline differences deserves careful consideration. Kim et al. (46) showed that 40 Hz ASSR impairments in ScZ patients could only be found when the data were not baseline-normalized, suggesting that higher noise-levels may be present. In addition, the involvement of brain regions beyond auditory cortex, such as the thalamus, hippocampus and frontal regions, is not reflected in the large majority of current EEG/MEG-studies. Given the extensive contribution of extended cortical and subcortical networks towards the generation of 40 Hz ASSRs (12, 18, 108), future analytic protocols should ideally apply whole-brain source-localization approaches. A recent study by Grent-'t-Jong et al. (12), for example, showed that specifically subcortical generators in the thalamus and hippocampus were strongly impaired in CHR-P and FEP groups and that reduced 40 Hz ASSRs in the thalamus predicted transition to psychosis in CHR-P participants.

Finally, given that 40 Hz ASSRs reflect E/I-balance parameters and that deficits in ITPC and spectral power may constitute a transdiagnostic biomarker, future studies could examine 40 Hz ASSRs across ScZ, BP and ASDs to define potentially novel illness subtypes (109) involving E/I-balance parameters.

Summary

The available evidence suggests that 40 Hz ASSRs are a promising biomarker, which is robustly impaired in ScZ patients across different paradigms and recording modalities (9, 10). In addition, test-retest reliability has been established in several studies (110, 111). Importantly, there is also emerging evidence that both CHR-P and FEP-groups are characterized by similar impairments in ITPC and spectral power during 40 Hz stimulation (12, 49) that could be potentially relevant for early detection and diagnosis. Developmental data furthermore indicate that 40 Hz ASSRs and the underlying generating mechanisms undergo major modifications during adolescence (17, 83, 84), indicating a sensitive period for both risk factors but also intervention to correct circuit anomalies.

Moreover, the 40 Hz ASSR also fulfills the criteria for a translational and mechanistic biomarker. Data from animal work has shown that similar to findings obtained from EEG- and MEG-recordings in humans, 40 Hz ASSRs elicit similar perturbations in both spectral power and ITPC that can be linked to circuit mechanisms fundamentally implicated in ScZ, in particular GABAergic interneurons and NMDA-Rs. Together with computational modelling (97, 99), these data allow the testing of mechanistic hypotheses that could lead to the development of targeted and more effective interventions.

Acknowledgments

PJU was supported by project MR/L011689/1 from the Medical Research Council (MRC) and the ERA-NET project 01EW2007A. PJU and CM were both supported through the Einstein Stiftung Berlin (A-2020-613). PJU and MB received support through grant UH 208/4-1from the German Research Foundation (DFG).

Disclosures

PJU has received research support from Lilly and Lundbeck outside the submitted work. All other authors report no biomedical financial interests or potential conflicts of interest.

Figure Legends

Figure 1: 40 Hz ASSRs in in EEG/MEG-Data. A) 40 Hz auditory stimulation elicits steady-state responses (ASSRs) measurable with EEG/MEG. Illustrated are typical response patterns both in 40 Hz power (analyzed with Time-frequency analysis – TFA) and phase (analyzed with intertrial phase coherence – ITPC). In EEG recording, these responses can be observed over fronto-central regions, while in MEG they are localized over temporal regions. Neuronal activity originating from dipoles in auditory cortex produce such topographies and differences between methodologies reflect differences in electric and magnetic signal transmission.
B): 40 Hz ASSRss consist of early transient and late sustained activity: Illustrated are a typical neuronal ASSR responses of human recordings using MEG, depicted by ITPC-values and the averaged steady-state potential. The difference between the early onset and the late sustained activity are clearly visible.
C): Overview of generators involved in 40 Hz ASSRs from multimodal imaging studies using PET/fMRI/EEG/MEG and intracranial recordings.

Figure 2: E/I-Balance Mechanisms of 40 Hz ASSRs and ScZ-associated Microcircuit Alterations: A) 40 Hz ASSRs are generated through the interaction between populations of

460 excitatory pyramidal cells (PC) and PV+ interneurons, which can be subdivided into two
461 groups, basket cells (PV B) and chandelier cells (PV C). Schizophrenia-associated changes
462 mainly occur at NMDA receptors at PC-PV synapses (1.) and PV-PC synapses (2. and 3.).
463 B) Simulated Circuit Parameters and 40 Hz ASSRs Deficits in ScZ: Six ScZ-associated network
464 parameters (GABA levels at pyramidal cells, GABA levels at inhibitory cells, number of
465 inhibitory connections to pyramidal cells, number of inhibitory connections to inhibitory cells,
466 prolonged GABAergic time constant at pyramidal cells, prolonged GABAergic time constant
467 at inhibitory cells) were changed in a computational model and the network response to 40 Hz
468 click trains was simulated. The panel shows the normalized mutual information between these
469 GABAergic network parameters and a 40 Hz ASSR power reduction (Inset: Mean and standard
470 deviation for the number of changed parameters), demonstrating that only a combination of
471 several parameters but not single parameters predicted 40 Hz ASSR power reductions (Figure
472 modified from Metzner et al. (37)) C/D.) Computational Modelling of PV-Interneuron Subtypes
473 and 40 Hz ASSRs in ScZ: Chandelier cells at a realistic ratio (10% of PV interneurons) do not
474 contribute significantly to the 40 Hz ASSR deficit. Basket cells are predominantly responsible
475 for the power reduction (Metzner et al. (97)). Simulated MEG signal (*left*) and resulting power
476 spectral density (*right*) for 40 Hz ASSR. The black curves represent the control model
477 configuration the red curves represent changes to the GABAergic system at chandelier cells
478 associated with schizophrenia.
479 D: Simulated MEG signal (*left*) and resulting power spectral density (*right*) for 40 Hz ASSR.
480 The black curves represent the control model configuration the red curves represent changes to
481 the GABAergic system at basket cells associated with schizophrenia. Only the basket cell
482 changes are able to significantly reduce the 40 Hz ASSR power.
483
484 **Figure 3: 40 Hz ASSRs and Clinical Outcomes in Early-Stage Psychosis.** Overview of
485 MEG-recorded 40 Hz ASSR mpairments in FEP-patients and CHR-P individuals: A) Source-

reconstructed ITPC activity in right Heschl‘s gyrus (RHES) for healthy control participants (HC: top time-frequency plot). B) 40-Hz ITPC traces for RHES in HC (black), CHR-P (blue) and FEPs (red) groups. C) Regions of interest for which virtual channel data were computed and statistically examined for group differences (RHES: right Heschl‘s gyrus, RTHA: right Thalamus, RHIP: right Hippocampus, RSTG: right Superior Temporal Gyrus). D) Cumming estimation plots with data distribution swarm plots and group difference data, including HCs and FEP-patients and three subgroups of CHR-P participants, based on 1-year follow-up data: APS-NP = non-persistent (remitted) attenuated psychotic symptoms (APS), APS-P = persistent APS, CHR-P-T = CHR-P who transitioned during follow-up time (up to 36 months). Linear Discriminant Analysis (LDA) predict clinical outcomes of CHR-P individuals based on MEG data Classification persistent APS vs. non-persistent APS: RHIP, RMTG, and RSTG ITPC: AUC = .845. A cross-validated total of 27 of 39 APS-NP (69.2%) and 25 of 34 APS-P (73.5%) participants were correctly classified. Classification CHR-P-T vs. CHR-P-NT (non-transitioned): RTHA: AUC = 0.695. A cross-validated total of 52 of 97 CHR-P-NT (53.6%) and 10 of 13 CHR-P-T (76.9%) participants was correctly classified for these two subgroups. These plots show predictive value of 40 Hz ASSR in AR groups for poor clinical outcome (adapted from Grent-‘t-Jong et al. (12)).

Figure 4: 40 Hz ASSRs in 22q11.2 Deletion Syndrome: A) Intertrial phase coherence (ITPC) values in EEG-data from control participants (n=48) and n=58 22q11.2 deletion carriers. The outlined dotted boxes highlight the time window of statistically significant group differences in gamma-band ITPC obtained from fronto-central electrodes. Power values are expressed in percent (Top Panel). Bottom Panel: Regions in source space (left and right ACC and superior frontal gyrus, right auditory cortex) with statistically significant lower gamma-band response (38–42 Hz) in deletion carriers (n=58) compared to healthy controls (n=48) during the first 1.5

sec of the 40 Hz ASSR. B) Differences in ITPC between 22q11.2 Deletion carriers with and without psychotic symptoms as defined by a score of 3 or more on the positive scale of the Structured Interview for Prodromal Syndromes (SIPS). Deletion group with psychotic symptoms was characterized by a statistically reduction in 40 Hz ASSR ITPC over the entire stimulation period (Top Panel). Bottom Panel: Correlations between gamma-band power over frontal electrodes and scores on the item P4 (Perceptual Abnormalities/Hallucinations) from SIPS (hallucinations). Power values are expressed in percent. C) 40 Hz ASSR spectral power during development (childhood, adolescence, and adulthood) in controls (top panel) and 22q11.2 deletion carriers (bottom panel). Spectral power is averaged across fronto-central electrodes and power values are expressed in percent. In controls, there is a significant increase in 38-42 Hz power during adolescence and adulthood which is absent in the 22q11.2 deletion group.

538 **References**

539

540 1. Kraguljac NV, McDonald WM, Widge AS, Rodriguez CI, Tohen M, Nemeroff CB
541 (2021): Neuroimaging Biomarkers in Schizophrenia. *Am J Psychiatry*. 178:509-521.
542 2. Wang B, Zartaloudi E, Linden JF, Bramon E (2022): Neurophysiology in psychosis:
543 The quest for disease biomarkers. *Transl Psychiatry*. 12:100.
544 3. Picton TW, John MS, Dimitrijevic A, Purcell D (2003): Human auditory steady-state
545 responses. *Int J Audiol*. 42:177-219.
546 4. Herrmann CS (2001): Human EEG responses to 1-100 Hz flicker: resonance phenomena
547 in visual cortex and their potential correlation to cognitive phenomena. *Exp Brain Res*. 137:346-
548 353.
549 5. Kwon JS, O'Donnell BF, Wallenstein GV, Greene RW, Hirayasu Y, Nestor PG, et al.
550 (1999): Gamma frequency-range abnormalities to auditory stimulation in schizophrenia. *Arch*
551 *Gen Psychiatry*. 56:1001-1005.
552 6. Uhlhaas PJ, Singer W (2010): Abnormal neural oscillations and synchrony in
553 schizophrenia. *Nat Rev Neurosci*. 11:100-113.
554 7. Singer W, Gray CM (1995): Visual feature integration and the temporal correlation
555 hypothesis. *Annu Rev Neurosci*. 18:555-586.
556 8. Uhlhaas PJ, Singer W (2015): Oscillations and neuronal dynamics in schizophrenia: the
557 search for basic symptoms and translational opportunities. *Biol Psychiatry*. 77:1001-1009.
558 9. Thune H, Recasens M, Uhlhaas PJ (2016): The 40-Hz Auditory Steady-State Response
559 in Patients With Schizophrenia: A Meta-analysis. *JAMA Psychiatry*. 73:1145-1153.
560 10. Onitsuka T, Tsuchimoto R, Oribe N, Spencer KM, Hirano Y (2022): Neuronal
561 imbalance of excitation and inhibition in schizophrenia: a scoping review of gamma-band
562 ASSR findings. *Psychiatry Clin Neurosci*. 76:610-619.

11. Tada M, Kirihara K, Koshiyama D, Fujioka M, Usui K, Uka T, et al. (2020): Gamma-Band Auditory Steady-State Response as a Neurophysiological Marker for Excitation and Inhibition Balance: A Review for Understanding Schizophrenia and Other Neuropsychiatric Disorders. *Clin EEG Neurosci*. 51:234-243.

12. Grent-'t-Jong T, Gajwani R, Gross J, Gumley AI, Krishnadas R, Lawrie SM, et al. (2021): 40-Hz Auditory Steady-State Responses Characterize Circuit Dysfunctions and Predict Clinical Outcomes in Clinical High-Risk for Psychosis Participants: A Magnetoencephalography Study. *Biol Psychiatry*. 90:419-429.

13. Spencer KM, Salisbury DF, Shenton ME, McCarley RW (2008): Gamma-band auditory steady-state responses are impaired in first episode psychosis. *Biol Psychiatry*. 64:369-375.

14. Farahani ED, Wouters J, van Wieringen A (2021): Brain mapping of auditory steady-state responses: A broad view of cortical and subcortical sources. *Hum Brain Mapp*. 42:780-796.

15. Herdman AT, Wollbrink A, Chau W, Ishii R, Ross B, Pantev C (2003): Determination of activation areas in the human auditory cortex by means of synthetic aperture magnetometry. *Neuroimage*. 20:995-1005.

16. Koshiyama D, Miyakoshi M, Joshi YB, Nakanishi M, Tanaka-Koshiyama K, Sprock J, et al. (2021): Source decomposition of the frontocentral auditory steady-state gamma band response in schizophrenia patients and healthy subjects. *Psychiatry Clin Neurosci*. 75:172-179.

17. Mancini V, Rochas V, Seeber M, Roehri N, Rihs TA, Ferat V, et al. (2022): Aberrant Developmental Patterns of Gamma-Band Response and Long-Range Communication Disruption in Youths With 22q11.2 Deletion Syndrome. *Am J Psychiatry*. 179:204-215.

18. Tada M, Kirihara K, Ishishita Y, Takasago M, Kunii N, Uka T, et al. (2021): Global and Parallel Cortical Processing Based on Auditory Gamma Oscillatory Responses in Humans. *Cereb Cortex*. 31:4518-4532.

588 19. Steinmann I, Gutschalk A (2011): Potential fMRI correlates of 40-Hz phase locking in
589 primary auditory cortex, thalamus and midbrain. *Neuroimage*. 54:495-504.
590 20. Delorme A, Makeig S (2004): EEGLAB: an open source toolbox for analysis of single-
591 trial EEG dynamics including independent component analysis. *J Neurosci Methods*. 134:9-21.
592 21. Reyes SA, Salvi RJ, Burkard RF, Coad ML, Wack DS, Galantowicz PJ, et al. (2004):
593 PET imaging of the 40 Hz auditory steady state response. *Hear Res*. 194:73-80.
594 22. Sukov W, Barth DS (2001): Cellular mechanisms of thalamically evoked gamma
595 oscillations in auditory cortex. *J Neurophysiol*. 85:1235-1245.
596 23. Ding N, Simon JZ (2009): Neural representations of complex temporal modulations in
597 the human auditory cortex. *J Neurophysiol*. 102:2731-2743.
598 24. Ozdamar O, Bohorquez J, Ray SS (2007): P(b)(P(1)) resonance at 40 Hz: effects of high
599 stimulus rate on auditory middle latency responses (MLRs) explored using deconvolution. *Clin*
600 *Neurophysiol*. 118:1261-1273.
601 25. Presacco A, Bohorquez J, Yavuz E, Ozdamar O (2010): Auditory steady-state responses
602 to 40-Hz click trains: relationship to middle latency, gamma band and beta band responses
603 studied with deconvolution. *Clin Neurophysiol*. 121:1540-1550.
604 26. An KM, Shim JH, Kwon H, Lee YH, Yu KK, Kwon M, et al. (2022): Detection of the
605 40 Hz auditory steady-state response with optically pumped magnetometers. *Sci Rep*. 12:17993.
606 27. Uhlhaas PJ, Singer W (2012): Neuronal dynamics and neuropsychiatric disorders:
607 toward a translational paradigm for dysfunctional large-scale networks. *Neuron*. 75:963-980.
608 28. van Bree S, Alamia A, Zoefel B (2022): Oscillation or not-Why we can and need to
609 know (commentary on Doelling and Assaneo, 2021). *Eur J Neurosci*. 55:201-204.
610 29. Donoghue T, Haller M, Peterson EJ, Varma P, Sebastian P, Gao R, et al. (2020):
611 Parameterizing neural power spectra into periodic and aperiodic components. *Nat Neurosci*.
612 23:1655-1665.

30. Buzsaki G, Wang XJ (2012): Mechanisms of gamma oscillations. *Annu Rev Neurosci*. 35:203-225.

31. Cardin JA (2016): Snapshots of the Brain in Action: Local Circuit Operations through the Lens of gamma Oscillations. *J Neurosci*. 36:10496-10504.

32. Whittington MA, Traub RD, Jefferys JG (1995): Synchronized oscillations in interneuron networks driven by metabotropic glutamate receptor activation. *Nature*. 373:612-615.

33. Wang XJ, Buzsaki G (1996): Gamma oscillation by synaptic inhibition in a hippocampal interneuronal network model. *J Neurosci*. 16:6402-6413.

34. Petilla Interneuron Nomenclature G, Ascoli GA, Alonso-Nanclares L, Anderson SA, Barrionuevo G, Benavides-Piccione R, et al. (2008): Petilla terminology: nomenclature of features of GABAergic interneurons of the cerebral cortex. *Nat Rev Neurosci*. 9:557-568.

35. Vierling-Claassen D, Cardin JA, Moore CI, Jones SR (2010): Computational modeling of distinct neocortical oscillations driven by cell-type selective optogenetic drive: separable resonant circuits controlled by low-threshold spiking and fast-spiking interneurons. *Front Hum Neurosci*. 4:198.

36. Vierling-Claassen D, Siekmeier P, Stufflebeam S, Kopell N (2008): Modeling GABA alterations in schizophrenia: a link between impaired inhibition and altered gamma and beta range auditory entrainment. *J Neurophysiol*. 99:2656-2671.

37. Metzner C, Schweikard A, Zurowski B (2016): Multifactorial Modeling of Impairment of Evoked Gamma Range Oscillations in Schizophrenia. *Front Comput Neurosci*. 10:89.

38. Kirli KK, Ermentrout GB, Cho RY (2014): Computational study of NMDA conductance and cortical oscillations in schizophrenia. *Front Comput Neurosci*. 8:133.

39. Carlen M, Meletis K, Siegle JH, Cardin JA, Futai K, Vierling-Claassen D, et al. (2012): A critical role for NMDA receptors in parvalbumin interneurons for gamma rhythm induction and behavior. *Mol Psychiatry*. 17:537-548.

639 40. Plourde G, Baribeau J, Bonhomme V (1997): Ketamine increases the amplitude of the
640 40-Hz auditory steady-state response in humans. *Br J Anaesth*. 78:524-529.
641 41. Wang X, Li Y, Chen J, Li Z, Li J, Qin L (2020): Aberrant Auditory Steady-State
642 Response of Awake Mice After Single Application of the NMDA Receptor Antagonist MK-
643 801 Into the Medial Geniculate Body. *Int J Neuropsychopharmacol*. 23:459-468.
644 42. Sivarao DV, Chen P, Senapati A, Yang Y, Fernandes A, Benitex Y, et al. (2016): 40 Hz
645 Auditory Steady-State Response Is a Pharmacodynamic Biomarker for Cortical NMDA
646 Receptors. *Neuropsychopharmacology*. 41:2232-2240.
647 43. Vohs JL, Chambers RA, Krishnan GP, O'Donnell BF, Berg S, Morzorati SL (2010):
648 GABAergic modulation of the 40 Hz auditory steady-state response in a rat model of
649 schizophrenia. *Int J Neuropsychopharmacol*. 13:487-497.
650 44. Hwang E, Brown RE, Kocsis B, Kim T, McKenna JT, McNally JM, et al. (2019):
651 Optogenetic stimulation of basal forebrain parvalbumin neurons modulates the cortical
652 topography of auditory steady-state responses. *Brain Struct Funct*. 224:1505-1518.
653 45. Hamm JP, Gilmore CS, Clementz BA (2012): Augmented gamma band auditory steady-
654 state responses: support for NMDA hypofunction in schizophrenia. *Schizophr Res*. 138:1-7.
655 46. Kim S, Jang SK, Kim DW, Shim M, Kim YW, Im CH, et al. (2019): Cortical volume
656 and 40-Hz auditory-steady-state responses in patients with schizophrenia and healthy controls.
657 *Neuroimage Clin*. 22:101732.
658 47. Koshiyama D, Miyakoshi M, Joshi YB, Molina JL, Tanaka-Koshiyama K, Joyce S, et
659 al. (2021): Neural network dynamics underlying gamma synchronization deficits in
660 schizophrenia. *Prog Neuropsychopharmacol Biol Psychiatry*. 107:110224.
661 48. Griskova-Bulanova I, Hubl D, van Swam C, Dierks T, Koenig T (2016): Early- and late-
662 latency gamma auditory steady-state response in schizophrenia during closed eyes: Does
663 hallucination status matter? *Clin Neurophysiol*. 127:2214-2221.

664 49. Tada M, Nagai T, Kirihara K, Koike S, Suga M, Araki T, et al. (2016): Differential
665 Alterations of Auditory Gamma Oscillatory Responses Between Pre-Onset High-Risk
666 Individuals and First-Episode Schizophrenia. *Cereb Cortex*. 26:1027-1035.
667 50. Roach BJ, Ford JM, Mathalon DH (2019): Gamma Band Phase Delay in Schizophrenia.
668 *Biol Psychiatry Cogn Neurosci Neuroimaging*. 4:131-139.
669 51. Roach BJ, Hirano Y, Ford JM, Spencer KM, Mathalon DH (2022): Phase Delay of the
670 40 Hz Auditory Steady-State Response Localizes to Left Auditory Cortex in Schizophrenia.
671 *Clin EEG Neurosci*.15500594221130896.
672 52. Tsuchimoto R, Kanba S, Hirano S, Oribe N, Ueno T, Hirano Y, et al. (2011): Reduced
673 high and low frequency gamma synchronization in patients with chronic schizophrenia.
674 *Schizophr Res*. 133:99-105.
675 53. Puvvada KC, Summerfelt A, Du X, Krishna N, Kochunov P, Rowland LM, et al. (2018):
676 Delta Vs Gamma Auditory Steady State Synchrony in Schizophrenia. *Schizophr Bull*. 44:378-
677 387.
678 54. Hamm JP, Gilmore CS, Picchetti NA, Sponheim SR, Clementz BA (2011):
679 Abnormalities of neuronal oscillations and temporal integration to low- and high-frequency
680 auditory stimulation in schizophrenia. *Biol Psychiatry*. 69:989-996.
681 55. Jensen O, Colgin LL (2007): Cross-frequency coupling between neuronal oscillations.
682 *Trends Cogn Sci*. 11:267-269.
683 56. Kirihara K, Rissling AJ, Swerdlow NR, Braff DL, Light GA (2012): Hierarchical
684 organization of gamma and theta oscillatory dynamics in schizophrenia. *Biol Psychiatry*.
685 71:873-880.
686 57. Murphy N, Ramakrishnan N, Walker CP, Polizzotto NR, Cho RY (2020): Intact
687 Auditory Cortical Cross-Frequency Coupling in Early and Chronic Schizophrenia. *Front*
688 *Psychiatry*. 11:507.

689 58. Coffman BA, Ren X, Longenecker J, Torrence N, Fishel V, Seebold D, et al. (2022):
690 Aberrant attentional modulation of the auditory steady state response (ASSR) is related to
691 auditory hallucination severity in the first-episode schizophrenia-spectrum. *J Psychiatr Res*.
692 151:188-196.
693 59. Spencer KM, Niznikiewicz MA, Nestor PG, Shenton ME, McCarley RW (2009): Left
694 auditory cortex gamma synchronization and auditory hallucination symptoms in schizophrenia.
695 *BMC Neurosci*. 10:85.
696 60. Ogyu K, Matsushita K, Honda S, Wada M, Tamura S, Takenouchi K, et al. (2023):
697 Decrease in gamma-band auditory steady-state response in patients with treatment-resistant
698 schizophrenia. *Schizophr Res*. 252:129-137.
699 61. Koshiyama D, Miyakoshi M, Thomas ML, Joshi YB, Molina JL, Tanaka-Koshiyama
700 K, et al. (2021): Unique contributions of sensory discrimination and gamma synchronization
701 deficits to cognitive, clinical, and psychosocial functional impairments in schizophrenia.
702 *Schizophr Res*. 228:280-287.
703 62. Hirano Y, Oribe N, Onitsuka T, Kanba S, Nestor PG, Hosokawa T, et al. (2020):
704 Auditory Cortex Volume and Gamma Oscillation Abnormalities in Schizophrenia. *Clin EEG*
705 *Neurosci*. 51:244-251.
706 63. Du X, Hare S, Summerfelt A, Adhikari BM, Garcia L, Marshall W, et al. (2023):
707 Cortical connectomic mediations on gamma band synchronization in schizophrenia. *Transl*
708 *Psychiatry*. 13:13.
709 64. Correll CU, Galling B, Pawar A, Krivko A, Bonetto C, Ruggeri M, et al. (2018):
710 Comparison of Early Intervention Services vs Treatment as Usual for Early-Phase Psychosis:
711 A Systematic Review, Meta-analysis, and Meta-regression. *JAMA Psychiatry*. 75:555-565.
712 65. McGorry P, Keshavan M, Goldstone S, Amminger P, Allott K, Berk M, et al. (2014):
713 Biomarkers and clinical staging in psychiatry. *World Psychiatry*. 13:211-223.

714 66. Koshiyama D, Kirihara K, Tada M, Nagai T, Fujioka M, Ichikawa E, et al. (2018):
715 Electrophysiological evidence for abnormal glutamate-GABA association following psychosis
716 onset. *Transl Psychiatry*. 8:211.
717 67. Wang J, Tang Y, Curtin A, Chan RCK, Wang Y, Li H, et al. (2018): Abnormal auditory-
718 evoked gamma band oscillations in first-episode schizophrenia during both eye open and eye
719 close states. *Prog Neuropsychopharmacol Biol Psychiatry*. 86:279-286.
720 68. Bartolomeo LA, Wright AM, Ma RE, Hummer TA, Francis MM, Visco AC, et al.
721 (2019): Relationship of auditory electrophysiological responses to magnetic resonance
722 spectroscopy metabolites in Early Phase Psychosis. *Int J Psychophysiol*. 145:15-22.
723 69. Lepock JR, Ahmed S, Mizrahi R, Gerritsen CJ, Maheandiran M, Drvaric L, et al. (2020):
724 Relationships between cognitive event-related brain potential measures in patients at clinical
725 high risk for psychosis. *Schizophr Res*. 226:84-94.
726 70. Ahmed S, Lepock JR, Mizrahi R, Bagby RM, Gerritsen CJ, Korostil M, et al. (2021):
727 Decreased Gamma Auditory Steady-State Response Is Associated With Impaired Real-World
728 Functioning in Unmedicated Patients at Clinical High Risk for Psychosis. *Clin EEG Neurosci*.
729 52:400-405.
730 71. Hilker R, Helenius D, Fagerlund B, Skytthe A, Christensen K, Werge TM, et al. (2018):
731 Heritability of Schizophrenia and Schizophrenia Spectrum Based on the Nationwide Danish
732 Twin Register. *Biol Psychiatry*. 83:492-498.
733 72. Trubetskoy V, Pardinas AF, Qi T, Panagiotaropoulou G, Awasthi S, Bigdeli TB, et al.
734 (2022): Mapping genomic loci implicates genes and synaptic biology in schizophrenia. *Nature*.
735 604:502-508.
736 73. Rass O, Forsyth JK, Krishnan GP, Hetrick WP, Klaunig MJ, Breier A, et al. (2012):
737 Auditory steady state response in the schizophrenia, first-degree relatives, and schizotypal
738 personality disorder. *Schizophr Res*. 136:143-149.

739 74. Metzner C, Maki-Marttunen T, Karni G, McMahon-Cole H, Steuber V (2022): The
740 effect of alterations of schizophrenia-associated genes on gamma band oscillations.
741 *Schizophrenia (Heidelb)*. 8:46.
742 75. Owen MJ, O'Donovan MC (2017): Schizophrenia and the neurodevelopmental
743 continuum:evidence from genomics. *World Psychiatry*. 16:227-235.
744 76. Gandal MJ, Zhang P, Hadjimichael E, Walker RL, Chen C, Liu S, et al. (2018):
745 Transcriptome-wide isoform-level dysregulation in ASD, schizophrenia, and bipolar disorder.
746 *Science*. 362.
747 77. Jefsen OH, Shtyrov Y, Larsen KM, Dietz MJ (2022): The 40-Hz auditory steady-state
748 response in bipolar disorder: A meta-analysis. *Clin Neurophysiol*. 141:53-61.
749 78. Seymour RA, Rippon G, Gooding-Williams G, Sowman PF, Kessler K (2020): Reduced
750 auditory steady state responses in autism spectrum disorder. *Mol Autism*. 11:56.
751 79. Larsen KM, Pellegrino G, Birknow MR, Kjaer TN, Baare WFC, Didriksen M, et al.
752 (2018): 22q11.2 Deletion Syndrome Is Associated With Impaired Auditory Steady-State
753 Gamma Response. *Schizophr Bull*. 44:388-397.
754 80. Schneider M, Debbane M, Bassett AS, Chow EW, Fung WL, van den Bree M, et al.
755 (2014): Psychiatric disorders from childhood to adulthood in 22q11.2 deletion syndrome:
756 results from the International Consortium on Brain and Behavior in 22q11.2 Deletion
757 Syndrome. *Am J Psychiatry*. 171:627-639.
758 81. Motahari Z, Moody SA, Maynard TM, LaMantia AS (2019): In the line-up: deleted
759 genes associated with DiGeorge/22q11.2 deletion syndrome: are they all suspects? *J Neurodev*
760 *Disord*. 11:7.
761 82. Meechan DW, Tucker ES, Maynard TM, LaMantia AS (2012): Cxcr4 regulation of
762 interneuron migration is disrupted in 22q11.2 deletion syndrome. *Proc Natl Acad Sci U S A*.
763 109:18601-18606.

764 83. Caballero A, Flores-Barrera E, Cass DK, Tseng KY (2014): Differential regulation of
765 parvalbumin and calretinin interneurons in the prefrontal cortex during adolescence. *Brain*
766 *Struct Funct*. 219:395-406.
767 84. Hashimoto T, Nguyen QL, Rotaru D, Keenan T, Arion D, Beneyto M, et al. (2009):
768 Protracted developmental trajectories of GABAA receptor alpha1 and alpha2 subunit
769 expression in primate prefrontal cortex. *Biol Psychiatry*. 65:1015-1023.
770 85. Renard J, Rushlow WJ, Laviolette SR (2018): Effects of Adolescent THC Exposure on
771 the Prefrontal GABAergic System: Implications for Schizophrenia-Related Psychopathology.
772 *Front Psychiatry*. 9:281.
773 86. Mukherjee A, Carvalho F, Eliez S, Caroni P (2019): Long-Lasting Rescue of Network
774 and Cognitive Dysfunction in a Genetic Schizophrenia Model. *Cell*. 178:1387-1402 e1314.
775 87. Curley AA, Lewis DA (2012): Cortical basket cell dysfunction in schizophrenia. *J*
776 *Physiol*. 590:715-724.
777 88. Javitt DC, Kantrowitz JT (2022): The glutamate/N-methyl-d-aspartate receptor
778 (NMDAR) model of schizophrenia at 35: On the path from syndrome to disease. *Schizophr Res*.
779 242:56-61.
780 89. Woo TU, Walsh JP, Benes FM (2004): Density of glutamic acid decarboxylase 67
781 messenger RNA-containing neurons that express the N-methyl-D-aspartate receptor subunit
782 NR2A in the anterior cingulate cortex in schizophrenia and bipolar disorder. *Arch Gen*
783 *Psychiatry*. 61:649-657.
784 90. Krystal JH, Anticevic A, Yang GJ, Dragoi G, Driesen NR, Wang XJ, et al. (2017):
785 Impaired Tuning of Neural Ensembles and the Pathophysiology of Schizophrenia: A
786 Translational and Computational Neuroscience Perspective. *Biol Psychiatry*. 81:874-885.
787 91. Krystal JH, Anticevic A (2015): Toward illness phase-specific pharmacotherapy for
788 schizophrenia. *Biol Psychiatry*. 78:738-740.

789 92. Jackson ME, Homayoun H, Moghaddam B (2004): NMDA receptor hypofunction
790 produces concomitant firing rate potentiation and burst activity reduction in the prefrontal
791 cortex. *Proc Natl Acad Sci U S A*. 101:8467-8472.
792 93. Rivolta D, Heidegger T, Scheller B, Sauer A, Schaum M, Birkner K, et al. (2015):
793 Ketamine Dysregulates the Amplitude and Connectivity of High-Frequency Oscillations in
794 Cortical-Subcortical Networks in Humans: Evidence From Resting-State
795 Magnetoencephalography-Recordings. *Schizophr Bull*. 41:1105-1114.
796 94. Pinault D (2008): N-methyl d-aspartate receptor antagonists ketamine and MK-801
797 induce wake-related aberrant gamma oscillations in the rat neocortex. *Biol Psychiatry*. 63:730-
798 735.
799 95. Hirano Y, Oribe N, Kanba S, Onitsuka T, Nestor PG, Spencer KM (2015): Spontaneous
800 Gamma Activity in Schizophrenia. *JAMA Psychiatry*. 72:813-821.
801 96. Grutzner C, Wibral M, Sun L, Rivolta D, Singer W, Maurer K, et al. (2013): Deficits in
802 high- (>60 Hz) gamma-band oscillations during visual processing in schizophrenia. *Front Hum*
803 *Neurosci*. 7:88.
804 97. Metzner C, Zurowski B, Steuber V (2019): The Role of Parvalbumin-positive
805 Interneurons in Auditory Steady-State Response Deficits in Schizophrenia. *Sci Rep*. 9:18525.
806 98. Metzner C, Steuber V (2021): The beta component of gamma-band auditory steady-
807 state responses in patients with schizophrenia. *Sci Rep*. 11:20387.
808 99. Adams RA, Pinotsis D, Tsirlis K, Unruh L, Mahajan A, Horas AM, et al. (2022):
809 Computational Modeling of Electroencephalography and Functional Magnetic Resonance
810 Imaging Paradigms Indicates a Consistent Loss of Pyramidal Cell Synaptic Gain in
811 Schizophrenia. *Biol Psychiatry*. 91:202-215.
812 100. Chung DW, Fish KN, Lewis DA (2016): Pathological Basis for Deficient Excitatory
813 Drive to Cortical Parvalbumin Interneurons in Schizophrenia. *Am J Psychiatry*. 173:1131-1139.

814 101. Siekmeier PJ, vanMaanen DP (2013): Development of antipsychotic medications with
815 novel mechanisms of action based on computational modeling of hippocampal neuropathology.
816 *PLoS One*. 8:e58607.
817 102. Tiitinen H, Sinkkonen J, Reinikainen K, Alho K, Lavikainen J, Naatanen R (1993):
818 Selective attention enhances the auditory 40-Hz transient response in humans. *Nature*. 364:59-
819 60.
820 103. Hamm JP, Bobilev AM, Hayrynen LK, Hudgens-Haney ME, Oliver WT, Parker DA, et
821 al. (2015): Stimulus train duration but not attention moderates gamma-band entrainment
822 abnormalities in schizophrenia. *Schizophr Res*. 165:97-102.
823 104. Griskova I, Morup M, Parnas J, Ruksenas O, Arnfred SM (2007): The amplitude and
824 phase precision of 40 Hz auditory steady-state response depend on the level of arousal. *Exp*
825 *Brain Res*. 183:133-138.
826 105. Griskova-Bulanova I, Ruksenas O, Dapsys K, Maciulis V, Arnfred SM (2011):
827 Distraction task rather than focal attention modulates gamma activity associated with auditory
828 steady-state responses (ASSRs). *Clin Neurophysiol*. 122:1541-1548.
829 106. Griskova-Bulanova I, Dapsys K, Maciulis V, Arnfred SM (2013): Closed eyes condition
830 increases auditory brain responses in schizophrenia. *Psychiatry Res*. 211:183-185.
831 107. Griskova-Bulanova I, Dapsys K, Melynyte S, Voicikas A, Maciulis V, Andruskevicius
832 S, et al. (2018): 40Hz auditory steady-state response in schizophrenia: Sensitivity to stimulation
833 type (clicks versus flutter amplitude-modulated tones). *Neurosci Lett*. 662:152-157.
834 108. Farahani ED, Goossens T, Wouters J, van Wieringen A (2017): Spatiotemporal
835 reconstruction of auditory steady-state responses to acoustic amplitude modulations: Potential
836 sources beyond the auditory pathway. *Neuroimage*. 148:240-253.
837 109. Clementz BA, Sweeney JA, Hamm JP, Ivleva EI, Ethridge LE, Pearlson GD, et al.
838 (2018): Identification of Distinct Psychosis Biotypes Using Brain-Based Biomarkers. *Focus*
839 *(Am Psychiatr Publ)*. 16:225-236.

840 110. Tan HR, Gross J, Uhlhaas PJ (2015): MEG-measured auditory steady-state oscillations
841 show high test-retest reliability: A sensor and source-space analysis. *Neuroimage*. 122:417-426.
842 111. Roach BJ, D'Souza DC, Ford JM, Mathalon DH (2019): Test-retest reliability of time-
843 frequency measures of auditory steady-state responses in patients with schizophrenia and
844 healthy controls. *Neuroimage Clin*. 23:101878.
845

Table 1. 40 Hz ASSR Studies in First-Episode Psychosis and Clinical-High Risk for Psychosis Participants

Study	Clinical Group	Age mean (SD)	Recording Technique	Stimulus Type	Main Results[a]
Ahmed et al., (69)	35 CHR	20.7 (3.4)	32-channel EEG	Click trains 40 Hz	---
Spencer et al. (13)	34 HC 16 FE-SZ 16 FE-AF	28 (8.7) 26 (8.1) 24 (7.4)	60-channel EEG	Click trains 20-, 30-, & 40-Hz 500 ms duration	FE-SZ < HC: power & ITPC FE-AF < HC: power & ITPC
Tada et al. (48)	21 HC 15 UHR 13 FES	22 (3.3) 22 (4.0) 25 (5.9)	64-channel EEG	Click trains 20-, 30-, & 40-Hz 500 ms duration	UHR < HC: only late latency power & ITPC FES < HC: early+late latency power & ITPC
Koshiyama et al. (65)	24 HC 27 UHR 21 ROSZ	22 (3.0) 21 (3.9) 24 (6.7)	64-channel EEG	Click trains 20-, 30-, & 40-Hz 500 ms duration	UHR < HC: only late latency power & ITPC ROSZ < HC: early+late latency power & ITPC
Wang et al. (66)	28 HC 33 FE	26 (5.5) 25 (6.6)	64-channel EEG	Click trains 40-Hz 500 ms duration	FE < HC: power & ITPC
Bartolomeo et al. (67)	19 HC 34 FE	22 (4.3) 23 (3.6)	28-channel EEG	Click trains 40-Hz 500 ms duration	FE = HC: power
Lepock et al. (68)	22 HC 36 CHR	22 (3.0) 21 (3.4)	32-channel EEG	Click trains 40-Hz 500 ms duration	CHR = HC: power & PLF
Grent-‘t-Jong et al. (12)	49 HC 38 CHR-N 116 CHR-P 33 FEP	23 (3.6) 23 (4.7) 22 (4.5) 24 (4.5)	248-channel MEG	AM sounds 40-Hz 2000 ms duration	CHR-P < HC: ITPC in RHES, power in RTHA and RHIP FEP < HC: power in RHES, RTHA and RHIP
Coffmann et al. (55)	32 HC 25 FE	24 (5.5) 24 (4.0)	63-channel EEG	Click trains 40-Hz 500 ms duration	FE = HC: power & ITPC

Abbreviations: HC = healthy controls; FE/FES/FEP = First-Episode Psychosis patients; FE-SZ and FE-AF = FEP schizophrenia and affective disorder, respectively; ROSZ = Recent Onset Schizophrenia patients; UHR = ultra-high risk participants; CHR = clinical high risk participant (CHR-P positive for psychosis risk, CHR-N negative for psychosis risk); SD = standard deviation of the mean; ms = milliseconds; AM = Amplitude Modulated sounds; ITPC = Inter-Trial-Phase-Coherence; RHES = right Heschl’s gyrus; RTHA = right Thalamus; RHIP = right Hippocampus.
[a] If more stimulation frequencies were presented, only the results from the 40-Hz stimulation condition are reported here.

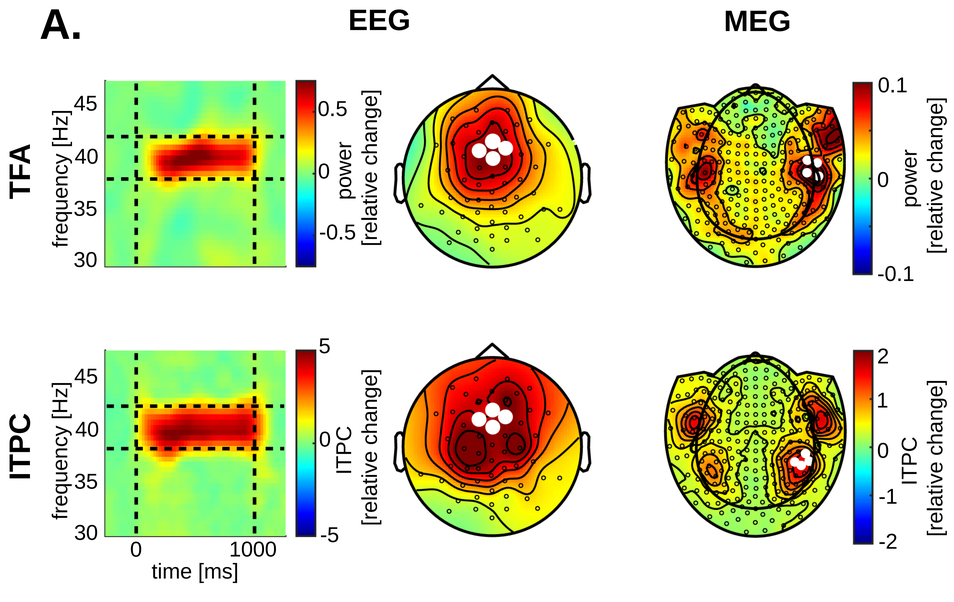

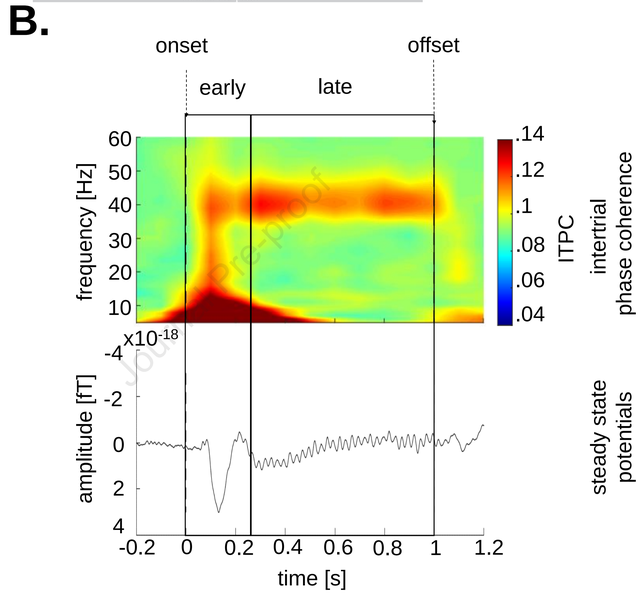

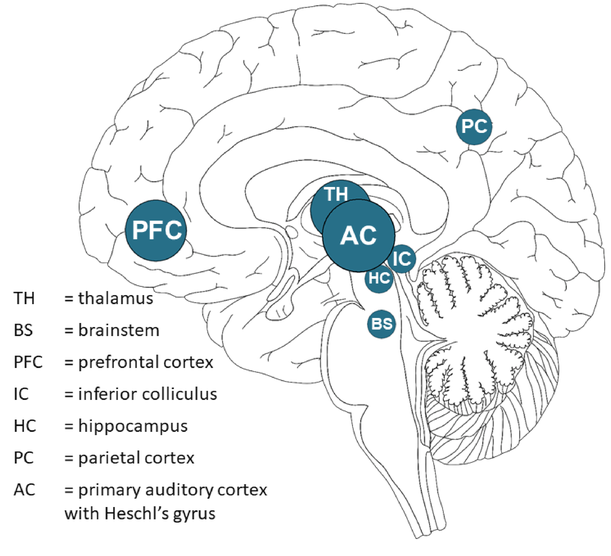

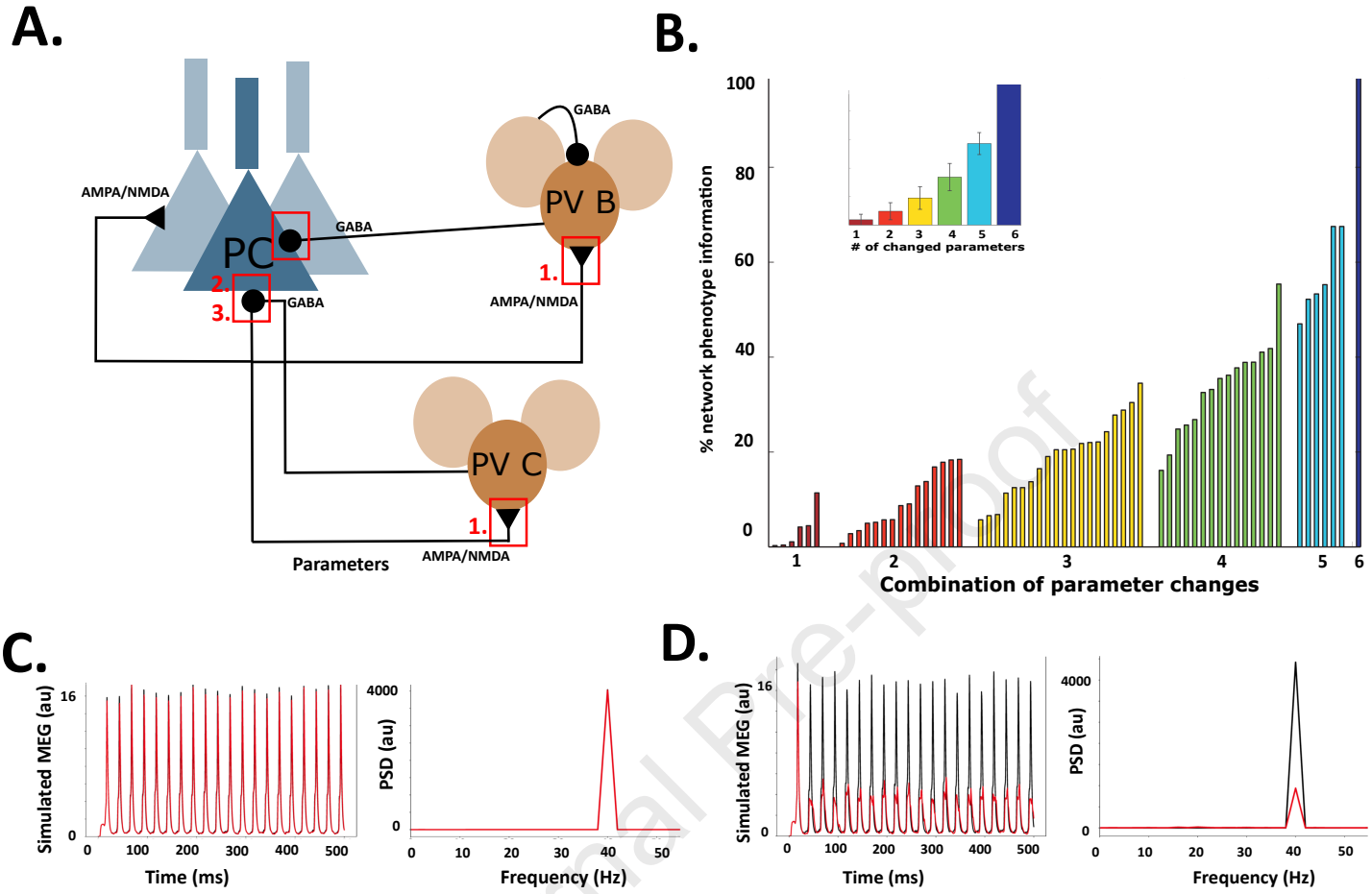

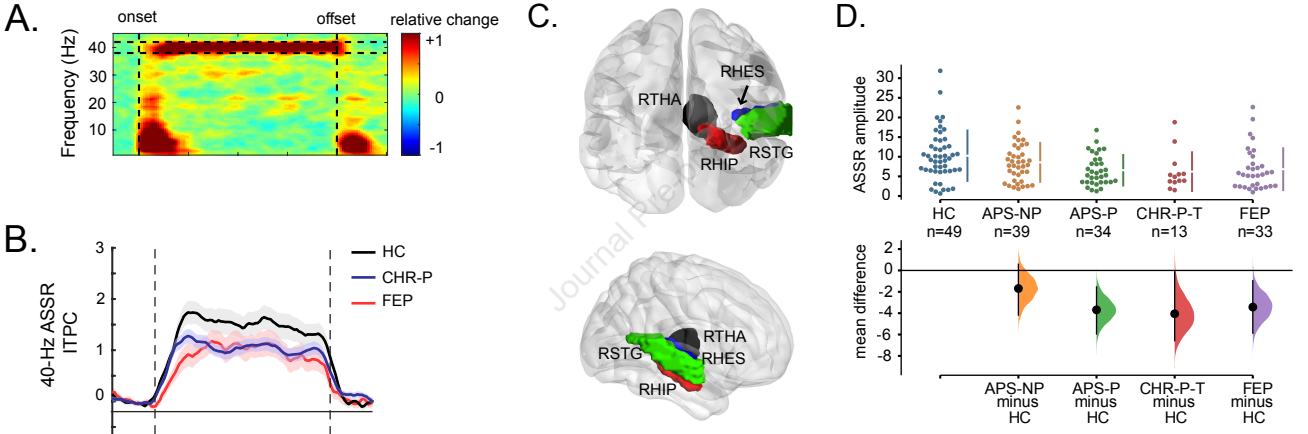

A

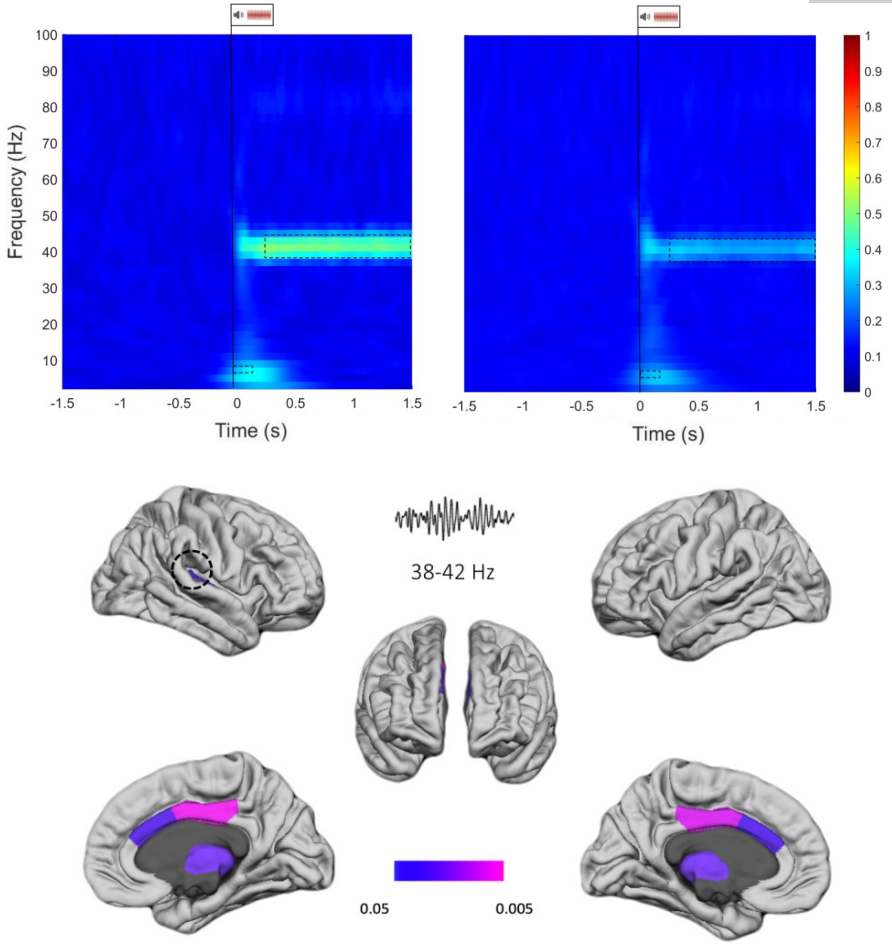

B

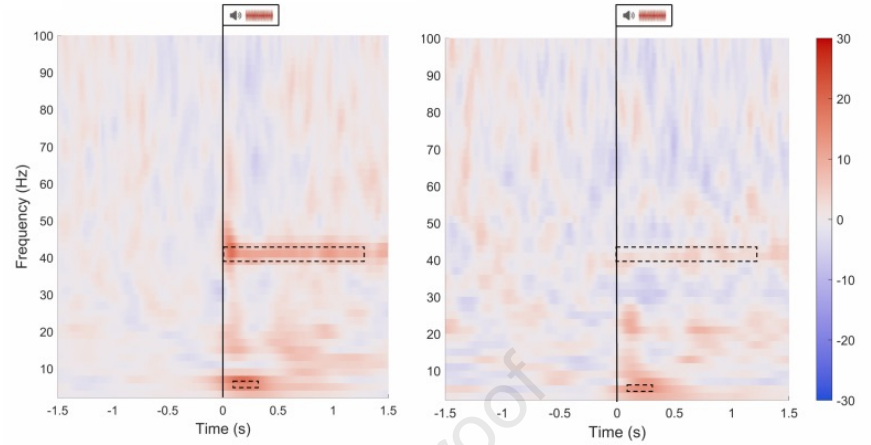

Correlation with psychotic symptoms

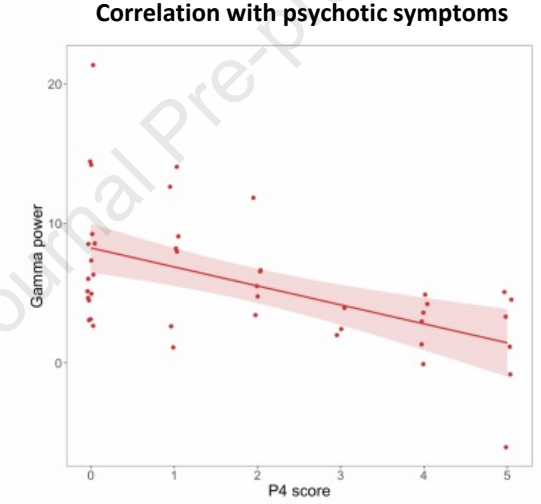

C